



## Linking Seawater Biogeochemistry to the Chemical and Biological Signatures of Nascent Marine Aerosol

Freney, Evelyn<sup>1</sup>, Sellegri, Karine<sup>1</sup>, Barthelmeß, Therese<sup>2</sup>, Engel, Anja<sup>2</sup>, Baumgardner, Darrel<sup>3</sup>, Hughes, Dagen<sup>3</sup>

5 <sup>1</sup>Université Clermont Auvergne, CNRS, Laboratoire de Météorologie Physique (LaMP), 63000 Clermont-Ferrand, France

<sup>2</sup>GEOMAR, Helmholtz Centre for Ocean Research Kiel, 24105 Kiel, Germany

<sup>3</sup>Droplet Measurement Technologies, LLC, Longmont, CO, USA

Contact author: evelyn.freney@cnrs.fr

### 10 **1.0 Abstract**

Interactions between the ocean and atmosphere are a key component in the Earth's climate system. Oceans represent an important source of aerosol particles in the atmosphere. However, uncertainties are still associated with our understanding of the complex processes involved in these interactions. This work presents a unique set of in-situ measurements focusing on the relationship between marine biogeochemistry and nascent marine aerosols over the Southern Ocean. These measurements were performed on nascent seawater aerosols generated, in an enclosed tank, from a continuous flow of seawater, during the Sea2Cloud cruise. This experimental set up provided the opportunity to study the interactions between the ocean and the atmosphere without the influence of background transported aerosols. These nascent seawater aerosols were characterised for their physical, biological, and chemical properties, using a combination of aerosol mass spectrometry and fluorescence spectroscopy. In parallel, detailed measurements of seawater biogeochemistry provided concentrations of different bacterial species, amino acids, and sugars in the seawater, enabling us to make links between organic aerosol types and seawater biochemistry.

Organic aerosol contributed 34-46% of the nascent sea spray. We observed that the contribution of oxidized organic aerosol dominated the nascent organic sea spray, indicating a large contribution of chemically or biologically processed organic matter already in the seawater. The contribution of organic material was highest at the start of the campaign in biologically active waters (>40%) and decreased to <40% later in the campaign. The contributions of the different type of OA changed across the seawater types showing that a marine OA evolves with the biogeochemical composition of seawater. The POA signature in the nascent sea spray was suspected to be less of a signature of biological debris and more representative of the biologically refractory and aged background organic matter of the ocean. The fluorescent aerosol particles (FAP) were logically proportional to most microorganism cell numbers but represented only 3% of the total aerosol nascent sea spray, and less than 10% of the total organic matter. Among these fluorescing particles, type A dominated with correlations with MOA, bacteria, but also with nanophytoplankton, diatoms and in general to total Chl-a. Classes B and C were uncorrelated to any microorganism but instead were sensitive to the presence of OOA and to a lesser extend MOA.



## 35 2.0 Introduction

Sea spray aerosol particles contribute a significant amount to the atmospheric aerosol population with estimated values of up to 6 kt y<sup>-1</sup> (Lewis and Schwatz, 2004) and can have direct radiative impacts ranging from 0 to -2 W/m<sup>2</sup> (Lohmann and Lesins, 2002). Depending on the geographical location, these particles can contribute significantly to the aerosol population and therefore have important impacts on cloud formation, atmospheric  
40 chemistry and radiative processes. Marine aerosol particles are known to be particularly efficient CCN (Ovadnevaite et al., 2011a) and can also act as ice nuclei (Wilson et al., 2015), these properties are believed to be enhanced when the biological content of these marine aerosols increased.

During wave breaking and wind processes, seawater droplets are released into the atmosphere and once evaporated, leave behind primary sea spray particles (Bigg and Leck et al., 2008), which are a mixture of inorganic and organic  
45 compounds. Recent studies during pristine ambient measurements have drawn our attention to the presence of both primary and secondary organic aerosol particles (Ovadnevaite et al., 2011, Chevassus et al., 2025)). These primary sea water particles range in diameter from less than 10 nm up to several microns (Sellegrri et al., 2023a). Given the small size of these particles, they can remain suspended in the air, and can be transported over large distances, and contribute to cloud condensation nuclei, thereby impacting aerosol indirect effects. These primary organic aerosols  
50 are composed of a complex mixture of sugars, amino acids (Decesari et al., 2020), and secondary organic aerosol particles are thought to be formed from the oxidation of marine volatile organic compounds such as dimethyl sulfide, or isoprene in the ambient air (Moore et al., 2024, Wohl et al., 2023, Chen et al., 2025).

The specific size and composition of these nascent seawater aerosol particles is dependent on several factors such as seawater composition, temperature, and wind speed (Sellegrri et al., 2023). We consider that these particles are  
55 generally composed of water-soluble salts such as sodium chloride and magnesium sulphate, but studies have now illustrated that submicron nascent sea spray aerosol particles may contain up to 70% of organic material (Ovadnevaite et al., 2011b). The presence of this organic matter in seawater can also influence the bubble bursting processes, notably their number and size distribution (Sellegrri et al., 2021). Additionally, the presence of certain organic compounds can impact the evaporation rates of aqueous droplets (Shulman et al., 1997) and others can  
60 slow down the hygroscopic growth of aerosol particles at relative humidity values of less than 100 %.

Given the importance of marine sources, an increasing number of studies have focused on characterizing marine aerosols. These are mostly performed in coastal environments (Ovadnevaite et al., 2011ab, Bearn et al., 2021), or  
65 as part of shipborne field campaigns (Schmale et al., 2019). Recently, new methods combining machine learning techniques with long-term measurements showed how specific periods of primary organic aerosols can be isolated and studied (Chen et al., 2025). Despite this, sources of other long-range transported aerosol particles are difficult to rule out.

In order to address this problem, field-based chamber approaches, which combine the control of laboratory experiments with naturel sampling environments have been deployed in a number of studies (Schwier et al., 2015,  
70 Wang et al. 2017, Freney et al., 2021). For studies focusing on marine aerosol particles, seawater is introduced into enclosed, particle-free chambers to generate nascent sea-salt particles. Depending on the objectives of the study, chambers are either supplied with discrete seawater samples collected at specific locations (Schwier et al., 2015), or with a continuous flow of seawater pumped directly from beneath a research vessel (Long et al., 2014, Freney et al., 2021, Frietas et al., 2022). These experimental setups enable the physical and chemical



75 characterisation of nascent seawater aerosols without interference from external atmospheric sources providing  
unique insights into their composition and the possibility to establish links to seawater biogeochemistry properties.  
Several such studies have demonstrated clear associations between aerosol chemical signatures and seawater  
biological activity. For example, primary marine organic aerosol (POA), were enriched during phytoplanktonic  
blooms (Wang et al., 2017). Wang et al. (2017) further showed that POA rapidly evolved into more oxidized  
80 organic aerosol in the presence of microbial activity, while Freney et al. (2021) identified specific mass spectral  
features tied to seawater biogeochemistry, including notable associations between slightly oxidized organic  
aerosol, containing methanesulphonique acid (MSA), and nanophytoplankton. The contribution of organic  
material to primary marine aerosols have additionally been observed using NMR experiments on sea spray aerosols  
(Descario et al., 2011, Dall'Osto et al., 2017) In all these studies, oxidised organic aerosol was already measured  
85 in the primary aerosol generation, which changes our perception of oxidised organic aerosols and their formation  
processes in marine environments.

Building on these previous studies on primary marine aerosols, we take a step further by characterising not only  
their chemical and physical properties but also their biological content. To achieve this, we incorporate online  
fluorescence measurements alongside conventional aerosol physical and chemical properties. Fluorescence  
90 spectroscopy has been shown to be particularly useful in identifying primary biological aerosol particles and are  
optimized to measure biological compounds such as tryptophan (TRY) and nicotinamide Adenine Dinucleotides  
phosphate (NADPH<sup>+</sup>), which are abundant in biological material (Savage et al., 2017). These techniques have  
been successfully applied in both laboratory and field campaigns, including deployment in challenging  
environments (Crawford et al., 2017). More recently, year-long measurements during the ACE 2017 experiment  
95 in the Southern Hemisphere demonstrated clear links between fluorescent particle concentrations, wind speed, and  
biological communities (Moallemi et al., 2021). Moallemi et al., (2021), reported positive relationships between  
fluorescent number concentrations and bacterial species, notably total bacteria and picoeukaryotes. However, like  
many measurement techniques, interference from organic aerosol particles other than biological species is  
common. For example, cigarette smoke, polycyclic aromatic compounds or humic acids can have similar  
100 properties to bacteria (Gabey et al., 2010, Hill et al., 1999). Highlighting the importance of using chamber systems  
to isolate nascent sea spray aerosol (SSA) particles from background airmasses, and to obtain a clean fluorescent  
signature that can be linked to nascent marine aerosols.

In this work, we first aim to illustrate the connection between ocean biogeochemistry and chemical and physical  
properties of nascent marine aerosols. Secondly, we seek to demonstrate the unique combination of aerosol mass  
105 spectrometry and fluorescence spectrometry to detect and characterise small nascent biological aerosol particles.  
Finally, we aim to identify distinctive fluorescent and mass spectral signatures that can be used as markers of  
nascent marine aerosol particles.

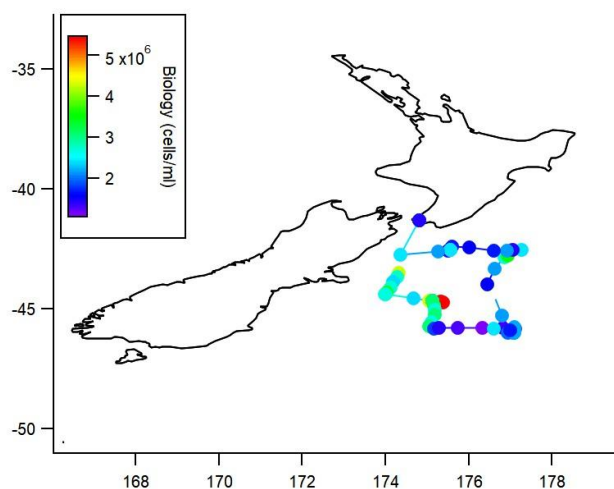
### 3.0 Methodology

#### 110 3.1 Cruise

The 2020 ship campaign Sea2Cloud took place from 15th to 27th March 2020, on board the research vessel (RV)  
Tangaroa from Wellington, New Zealand. The ship traveled between -42° and -46° latitudes, and 172° and 177°  
longitudes in the Northern Southern Ocean (Fig. 1). The ship was at its farthest point of the land on 23rd of March



2020. The sampled area was chosen as it is at the crossroads where sub Antarctic Sea waters traveling up North  
115 meet subtropical seawaters traveling down South. The oceans currents are influenced by the underwater  
topography of the Chatham Rise, the plateau east of NZ. The Chatham Rise is visibly enriched in Chl-a on satellite  
ocean color images. The details of the methodical approach used in the campaign are described in Sellegri at  
al.(2023b).



120 Figure 1: Ship transect during the field campaign. The transect is coloured by the number of biological cells  
measured in the water.

During the cruise, the ship encountered four different water types. The seawater salinity and temperature are used  
to distinguish the different water types during the sampling campaign according to the criteria defined by Chiswell  
125 et al (2015): Subantarctic waters (SAW) are defined by salinity lower than 34.5 g/L, Frontal waters (FW) by  
salinity between 34.5 and 34.8 g/L and Subtropical water (STW) by salinity greater than 34.8 g/L. Given the  
variability of salinity at the end of the campaign, a fourth water type as Mixed waters (MW) was additionally  
defined, corresponding to the mixture of subtropical and frontal waters.

130 Each type of seawater is described more thoroughly in Sellegri et al, (2023b). Briefly, frontal waters (FW) were  
sampled from 17<sup>th</sup> of March 11:00 to 20<sup>th</sup> of March 17:00 (NZ time), Subantarctic waters (SAW) from 20<sup>th</sup> of  
March 17:00 to 24<sup>th</sup> of March 04:00, and Subtropical waters (STW) from 24<sup>th</sup> of March 04:00 to 25<sup>th</sup> of March  
8:00. Mixed waters (MW) were encountered from 25<sup>th</sup> of March 8:00 to the end of the voyage on 27<sup>th</sup> of March  
00:00 (Figure S7). As will be discussed in more detail later in the manuscript, elevated biomass was sampled in  
135 frontal waters from 18<sup>th</sup> of March to the 20<sup>th</sup> of March, while the lowest biomass was observed in subantarctic  
waters between 20<sup>th</sup> of March and 23<sup>th</sup> of March. Low nutrient waters (total nitrate and phosphorus) were sampled  
in subtropical waters on 24<sup>th</sup> and 25<sup>th</sup> of March. Whereas SAW and MW were high in total nitrate concentrations.



### 3.2 Seawater sampling and nascent aerosol generation

140 Seawater samples were collected in a continuous (online) manner at a depth of 6 m using the underway system of the ship (UWAY), this sampling method was used for bulk seawater samples and for artificially generating natural Sea Spray Aerosols (SSA). Bulk seawater sampling was analyzed, using flow cytometry (FCM), various biogeochemical parameters including amino acids, combined carbohydrates, and bacterial cells, including prokaryotic, picophytoplankton, nanophytoplankton) at intervals of 4 to 8 hours.

145 Aerosols were measured from the artificially generated SSA produced continuously using the same method as described in Sellegrì et al., (2023a). Seawater was transported from under the ship (underway) at a depth of 5 meters. This seawater is continuously introduced into a 10-liter glass tank via a series of 1 mm nozzles; this process induces bubble formation at the seawater surface and mimics the process of breaking waves. SSA from these processes is then released into the particle-free air of the tank and is then sampled through a 1 m long silica gel diffusion drier. The physical properties of generated SSA flux were analysed using a scanning mobility particle sizer (SMPS, I LPM) measuring particle number concentration as a function of size from 10 to 500 nm. Total particle number concentration was measured using a condensation particle counter (MAGIC CPC, 0.3 LPM). Aerosol chemical properties were measured using a time-of-flight aerosol chemical speciation monitor (Aerodyne ToF-ACSM serial number: TACSM13). From a parallel line (35 cm long 1/2 inch) with no dryer, fluorescence properties of particles ranging from 500 nm up to 30 Microns were measured using the wideband integrated bioaerosol sensor (WIBS-5).  
150  
155

### 3.3 Instrumental description

#### 3.3.1 Aerosol chemical and physical properties

160 The TACSM used in this work was equipped with a PM1 inlet with a standard vaporizer (@ 600°C), meaning that only non-refractory materials were measured quantitatively manner. Like previous work (Freney et al., 2021) the standard fragmentation table for the Aerodyne ACSM was modified to include a sea salt species. Mass concentrations at m/z 58, 60, 81 and 83 were assigned to this seasalt species. The total PM1 sampled with the ToF-ACSM was on average  $1.77 \pm 1.5 \text{ ug m}^{-3}$  and was validated against mass concentrations measured using a Differential Mobility Particle Sizer (DMPS, custom made) coupled with a condensation particle counter (CPC, TSI, 3010). The agreement between the two instruments was good ( $r=0.73$ ,  $\text{slope}=0.82$ ), showing that little undetected refractory mass existed in the submicron mass concentration (Figure S1).  
165

Using only the organic aerosol mass spectra, positive matrix factorisation (PMF) was performed using the SOFI tool (Version 6B). Three factors were identified, like those already identified in Freney et al., (2021), with a nascent oxidized organic factor (OOA), a primary marine organic (POA) signature and a marine organic aerosol (MOA) spectrum. The results of the PMF analysis will be discussed later in section 4. A two-factor solution contained a mixed OOA solution where the marine associated peaks of the MOA were absorbed into the OOA (Fig S3). A four-factor solution led to the splitting of the factors with no additional information provided (Fig. S4).  
170



### 3.3.2 Particle fluorescence measurements

The WIBS-5 (Droplet Measurement Technologies LLC) instrument provided fluorescence measurements as a function of particle size in the range of 0.5 to 30  $\mu\text{m}$ . Given that during this field campaign the number concentrations of those particles greater than 15  $\mu\text{m}$  were low, the discussion is focused on particles with diameters from 0.5  $\mu\text{m}$  up to 15  $\mu\text{m}$ . This instrument provides fluorescent measurements for single particles using laser induced fluorescence (UV-LIF) (Savage et al., 2017). Aerosol particles are excited using two Xenon flash lamps at wavelengths 280 nm and 370 nm. These wavelengths are specific to the excitation wavelengths of TRY and NADPH fluorescence. The total fluorescence light intensity is measured in the range of 310 nm to 400 nm and from 420 nm to 650 nm specific to the emission spectrum of TRY and in the range of 420 nm to 650 nm for NADPH. This method allows us to distinguish biological aerosol particles from non-biological aerosols. The total flow rate of the WIBS-5 is set up at 2.5 L/min, and a lower sample flow of 0.23 L/min is split from this main flow. To provide a cross verification of the different instruments, we compared the  $\text{dN/dLog}(D_p)$  lower size channels of the WIBS instruments to those overlapping with that of the DMPS (Fig. S5). Considering the conversions of a mobility diameter to an optical diameter we compared the 710 nm size channel in the WIBS with that of the 500 nm size channel in the DMPS. Data was analysed using both the WIBS analysis Toolkit version 1.36 and Wibs data display).

The WIBS fluorescence signal was classified using the Perring classification (Perring et al. 2015). The classification is detailed in Table S2. In this study, we provided measurements at the detection threshold of  $3\delta$  Sigma (Modal peak plus 3 times the standard deviation), and at  $9\delta$ . The  $3\delta$  threshold provides information on all fluorescent particles; however, previous studies have illustrated that non-biological aerosol particles can sometimes fluoresce, and it is suggested to increase the fluorescence threshold to  $9\delta$  to remove fluorescence signals from non-biological particles. Using this threshold only highly (or hyper) fluorescent particles are selected. We calculate fluorescent fractions and ratios at both threshold values to provide a comparison with previous studies (Savage et al., 2017, Moallemi et al. 2021, Frietas et al., 2022).

## 4.0 Results and discussion:

### 4.1 General observations

#### 4.1.2 Overview of the variability of the biogeochemical parameters

Prior to going into detail on the chemical and physical properties of the nascent aerosol particles, we first present seawater biogeochemical parameters measured using the underway water system. These measurements provide an indicator of the biological activity in the water and will provide a basis for the interpretation of the properties of the generated aerosol particles. All relevant time series are provided in the supplementary material (Fig S6 S7). Chlorophyll-a (Chl-a) concentrations are highest in the FW, reaching approximately  $2 \text{ mg}\cdot\text{m}^{-3}$  (Fig S6a), with a peak of about  $4 \text{ mg}\cdot\text{m}^{-3}$  during a phytoplankton bloom observed on 19<sup>th</sup> of March. In contrast, Chl-a are lowest in the SAW and in the STW, ranging between  $0.2$  and  $0.5 \text{ mg}\cdot\text{m}^{-3}$ , and increases in the MW to about  $1 \text{ mg}\cdot\text{m}^{-3}$ . Total heterotrophic bacterial abundance (Bact), (Fig S6b) is also highest in the FW and MW, with brief periods of



elevated concentrations observed on 19<sup>th</sup> of March (FW), 23<sup>th</sup> of March (SAW) and 26<sup>th</sup> of March (MW). Nanophytoplanktons (Nano) (Fig. S5c), are most abundant in the FW and least in the MW, with intermediate  
210 values in the SAW. In contrast, picophytoplanktons (Pico) (Fig. S6c), show the lowest concentrations in the FW, but display high variability, peaking on 18<sup>th</sup> of March across all populations.

Bigger single-cell algae species, such as dinoflagellates (DiFl), diatoms (DiA) and flagellates (Fl), are highly variable throughout the sampling period (Fig. S7d). DiA exhibits peak concentrations in the FW, with concentrations tenfold those measured in the SAW and in the STW. DiFl are highest in the FW (20 mgC.m<sup>-3</sup>),  
215 average in the SAW/STW (15 mgC.m<sup>-3</sup>) and lowest in the MW (<10 mgC.m<sup>-3</sup>), while Fl is highest in the STW/MW and lowest in the SAW. Total nitrogen was highest in the SAW waters and lowest in the STW (as was other nutrients such as phosphorus).

To summarize, the FW had the highest biological activity and biomass, especially for larger phytoplankton groups and chlorophyll-a. The STW was generally low nutrient water but had highest temperature and salinity values, as  
220 well as the fractional abundance of some larger single-cell species (Flagellates) but generally was low nutrient water. The smaller phytoplanktons (Pico, Syn) showed an opposite trend, with higher biomass in the SAW. Dissolved Amino acid (AA) species, such as Glycine, Alanine, Gamma-aminobutyric acid (GABA), Isoleucine (Iso), Phenylalanine (Phe) and Leucine (Leu) were also measured in the water daily. The changes in these concentrations are relatively subtle but using a degradation index, it is possible to extract shifts in the molecular  
225 AA composition. This degradation index is calculated based on a principal component analysis (PCA) including all data from the Tangaroa voyage (ASIT, UW, and working boat) (Barthelmeß et al., 2025). This corresponds to a certain molecular composition i.e. a relative higher share of Gly, Ala, and GABA points to a higher state of degradation, while a higher relative share of e.g. Iso, Phe, and Leu point to fresh (recently produced) organic matter. From this analysis it is concluded that the MIX and FW contained the freshest organic matter, followed by  
230 SAW and then STW which was the most degraded and contained the least amount of fresh material.

#### 4.1.2 Aerosol chemical characterisation

The chemical composition measured by the TACSM included contributions from sea salt, SO<sub>4</sub><sup>2-</sup>, Org, and NO<sub>3</sub><sup>-</sup>. The average mass concentration of the organic species was 0.75 ± 0.78 µgm<sup>-3</sup>, accounting for approximately 35% ± 20% of the measured submicron particle mass concentrations (Fig. 2), slightly higher than the organic fractions  
235 measured during the Mediterranean Peacetime cruise (Freney et al., 2021). The contribution from SO<sub>4</sub><sup>2-</sup> is on average 11%±8% and 4%±8% from NO<sub>3</sub><sup>-</sup>. The sea salt aerosol contributes approximately 40%±20%. The ratio of the Sea salt signal to SO<sub>4</sub><sup>2-</sup> is on average 0.25, which is in accordance with literature values (0.26) citing the ionic composition of seawater (Seinfeld and Pandis (2016). Therefore, we believe that SO<sub>4</sub><sup>2-</sup> measured only represents the SO<sub>4</sub><sup>2-</sup> within naturel sea salt. The NO<sub>3</sub><sup>-</sup> measured was often close to the limit of detection, resulting in higher  
240 ratios (0.04) than those cited in the literature (0.0001). Given the difficulty in quantifying sea salt using the TACSM we do not discuss the sea salt composition further. Like the other physical and biological variables, the highest PM1 mass concentrations were observed during both the FW (2.34 ± 1.82 µg m<sup>-3</sup>) and the STW (1.94 ± 0.86 µg m<sup>-3</sup>) periods, compared with concentrations measured in the SAW (1.2 ± 0.74 µg m<sup>-3</sup>) and MW (0.835 ± 0.75 µg m<sup>-3</sup>).

245

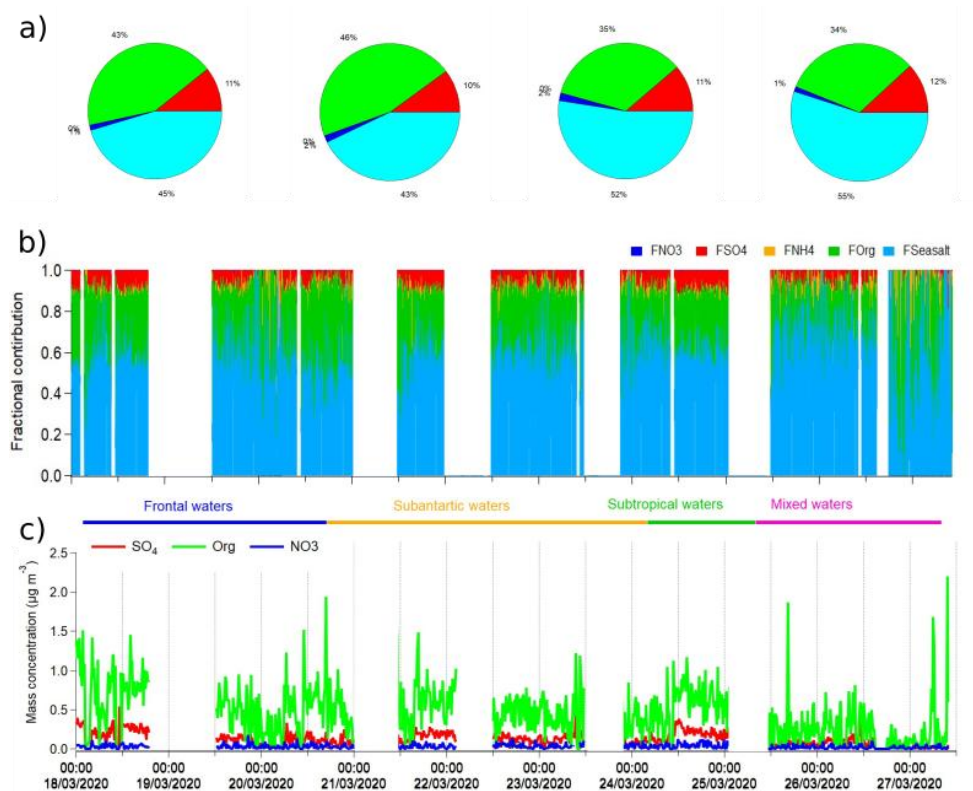


Figure 2. TACSM mass concentration of the Organic, Sulphate, and nitrate species as a function of time and water type.

250

Positive Matrix Factorization (PMF) was performed on the organic mass concentration, and a three-factor solution was chosen to best describe the dataset (Fig. 3). These factors represented a MOA, an OOA, and an POA, similar to signatures previously identified in Freney et al., (2021). The OOA (Fig.3 e) signature was typical of that of an oxidized organic aerosol, whereas the MOA had similar mass spectral fragments of the combined marine organic aerosol and methyl sulphonate acid (MSA) factors identified in Freney et al., (2021) having signature peaks of  $m/z$  65, 79, and 96. These peaks have been characterised in a number of studies and have been associated with an MSA-like organic aerosol (Timonen et al., 2016, Hodshire et al., 2019). The MOA factor additionally contained several mass spectral peaks that have previously been associated with amino acids groups such as  $m/z$  41, 70, 98, 117 (Schmale et al., 2013 (ambient marine aerosols) or Alfarra et al., 2004 (Palmitic and Oleic acid)).

260

The total organic mass fraction decreased from 43% in the FW to 34% in the STW and MX. This change in total organic matter was additionally accompanied by a change in the composition of organic aerosols with MOA contributing the highest to the total Org in the FW (50%), shows a stable relative contribution at 30% in SAW and STW, and a very low contribution of around 10% in MW. The OOA, however increases throughout the campaign, with about 40% of the total Org in FW, stable 50% in SAW and STW and 70% in MW. The POA contributes the least to the total organic mass, ( $10 \pm 5$  %), it is the only organic mass that had a constant contribution throughout

265



the field campaign, except for several short periods of higher concentrations around the 22nd of March. These peaks coincide with low overall mass concentrations, and we do not believe that they are resulting from a particular source.

270

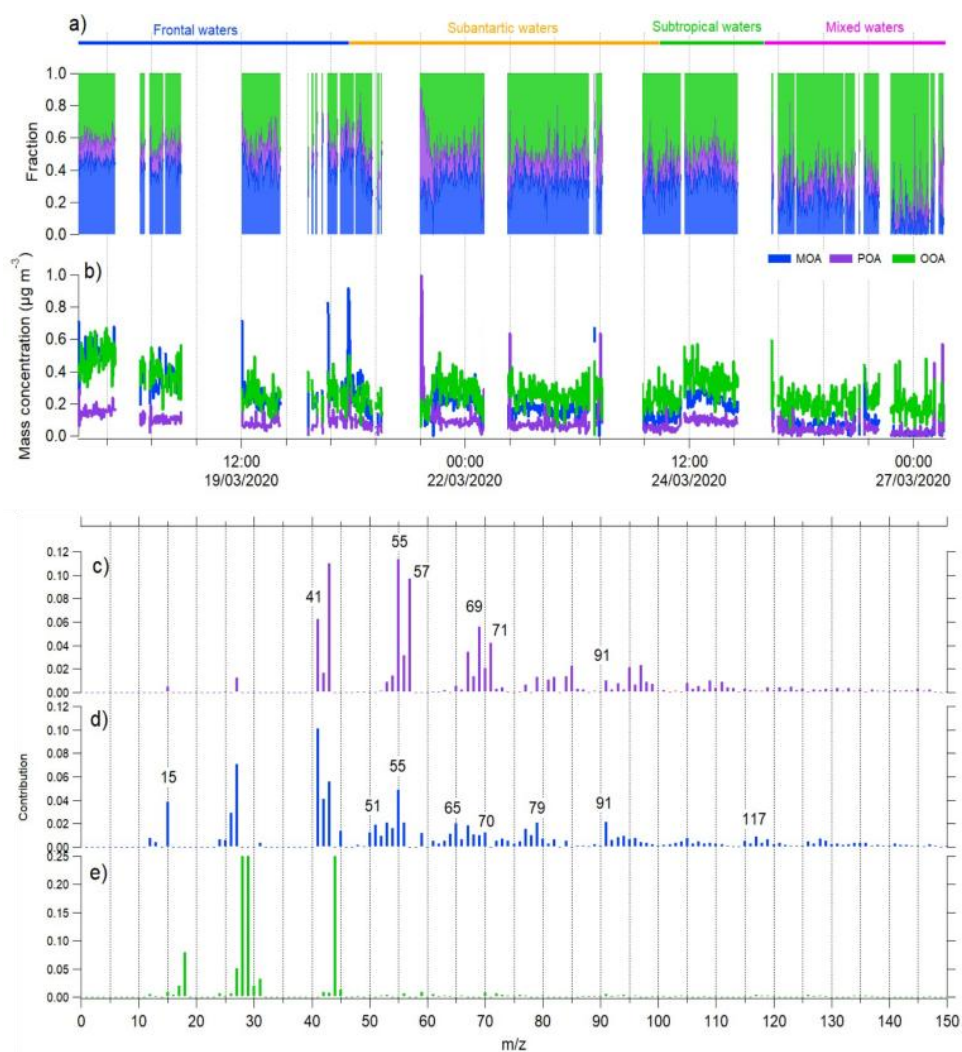


Figure 3: Top: a) Contribution of each of the OA, b) mass concentrations of the three identified organic factors c) MOA, d) POA and e) OOA as a function of time. The bottom figure illustrates the mass spectral profiles of each of the three identified factors.

275

In the current configuration, the residence time in the chamber is 30 seconds and does not allow for the formation of secondary aerosol from gas-phase precursors. Our observations of oxidized organic matter in nascent SSA confirm those from the peacetime Mediterranean cruise (Frey et al., 2021) and suggest that the oxidation of



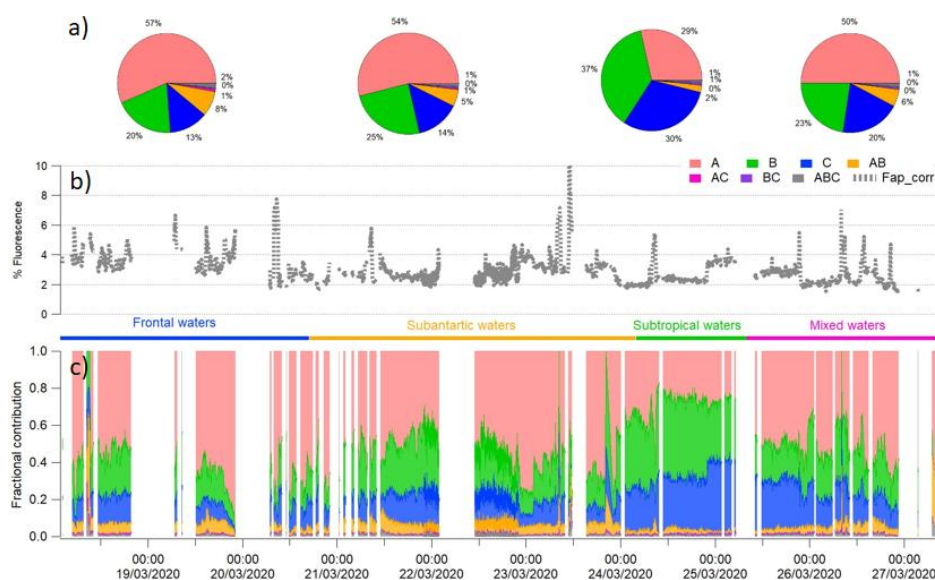
280 organic matter is already occurring in the bulk or at the surface of the seawater. MOA and OOA have been  
measured in ambient air over the North Atlantic (Decesari et al., 2011). Facchini et al., (2008) observed that  
chemical analysis of primary sea water aerosols was mainly composed of lipopolysaccharides that were transferred  
to the submicron aerosol during bubble bursting. Zhou et al (2008) also showed that primary marine organic  
aerosol can act as a source of OM but also a sink for the OH radical and lead to the production of low molecular  
285 weight organic compounds. Long et al., (2014), illustrated how solar radiation can impact the production of organic  
matter in seawater, through both biological and photochemical processes. These studies, along with our  
observations illustrate that nascent marine organic aerosols are a combination of nascent and secondary aerosol  
sources and highlights the need to reconsider the sources of secondary aerosol particles in marine environments.

### 1.3 Fluorescent properties

290 In this work a WIBS-NEO instrument was deployed as part of the instrumental set up to facilitate the link between  
seawater biochemistry and the biological content of nascent seawater aerosols. Our objective was to determine to  
what extent biological material was emitted into the atmosphere during nascent SSA generation. These online  
measurements, should allow us to study under what conditions of seawater biological properties result in the  
highest fluorescent aerosol particles and what are the fluorescent characteristics of these aerosol particles.

295  
Aerosol particle number and mass concentrations were measured, both by the DMPS (from 10 up to 500 nm) and  
the WIBS-5 (from 500 nm up to 15000 nm). Both instruments measured highest concentrations at the start of the  
field campaign, in the FW, and like the aerosol chemical properties an increase in number concentrations was  
observed during the STW. The aerosol size distribution measured by the DMPS was characterized by a single  
300 mode centered on 150 nm, and particle number concentrations measured by the WIBS-5 were dominated by  
particles with diameters < 2 microns (Fig. S4). A more detailed description of aerosol particle size distributions  
during the field campaign, as well as their variability with seawater temperature is available in Sellegri et al.,  
(2023b).

Of all particles sampled by the WIBS instrument, only 2 to 4% were fluorescent aerosol particles (FAP) at 3-sigma  
305 (Fig. 4), with highest FAP in FW. For the hyper fluorescent particles (HFP) (9-sigma), only 1% $\pm$  0.5% of the  
particles were fluorescent. This suggests that only a small fraction of the total aerosol and total organics (30%) is  
of biological origin. These values are like those reported for highly fluorescent nascent sea salt particles in the  
Baltic Sea (2022), and in ambient aerosols over the Pacific Ocean (Moaellimi et al., 2021). The disadvantage of  
using only this ABC channel to identify biological aerosol particles is that we likely miss useful information from  
310 the remaining channels. The FAP was highest in frontal waters (around 4%) and decreased throughout the  
campaign, was around 3% in SAW and only 2% in STW and MW, logically following the general trend of most  
phytoplankton groups.



315 Figure 4: a) Time series of the fluorescent particle number concentration, b) Time series of the contribution of each  
fluorescence channel (3 sigma) in each water type (indicated by the colored bars),

In this work, 90% of the FAP were particles that were fluorescing in single channels (A, B, and C), while mixed  
channels (AB, AC, BC, ABC) contributed less than 10% of all fluorescing particles (Fig.4). The A type particles  
320 contributed more than 40% during most of the field campaign. These particles are excited by 280 nm and emit in  
the range of 310 to 400 nm (Table S2).

In ambient aerosol measurements, the fluorescent particle types A, AB, in smaller size ranges have been associated  
with bacteria, whereas in larger particles this can eventually suggest the presence of fungal species. In STW, the  
fraction of A particles decreased to 29%, as a result of an increase in contributions from B and C particles, (37  
325 and 30% respectively). In all other water types, these B and C type particles ranged from 20 to 25% and from 13 to  
20%, respectively. During ambient measurements in marine environments, the B class particle fractions generally  
represent smaller contributions < 15%, (Kawana et al., 2015, Moallemi et al 2021). When looking at hyper  
fluorescent particles (9-sigma), the same trends in all channels were observed, however contributions from A  
decreased by approximately 20%, whereas those from the B and the C channels increased, suggesting a  
330 contribution of weakly fluorescing particles occurs in this A channel. B and C type particles can be related to  
biofluorophores such as riboflavin (Savage et al., 2017).

There was a notable variation in different fluorescent channels depending on the water type and measured particle  
size (Fig. S8). In the FW and in the STW, all measured particles represented similar fluorescent properties across  
the measured size range. However, in the SAW, the intensity of A type particles was particularly strong at smaller  
335 diameters. The fluorescent intensity in mixed waters showed the ABC channels with a marked increase at larger  
diameters.

Several recent studies have deployed the WIBS instrument aboard research vessels in the southern hemisphere and  
sampled in marine ambient air (Moallemi et al., 2021, Kawana et al., 2021). In the Baltic Sea, a fluorescence

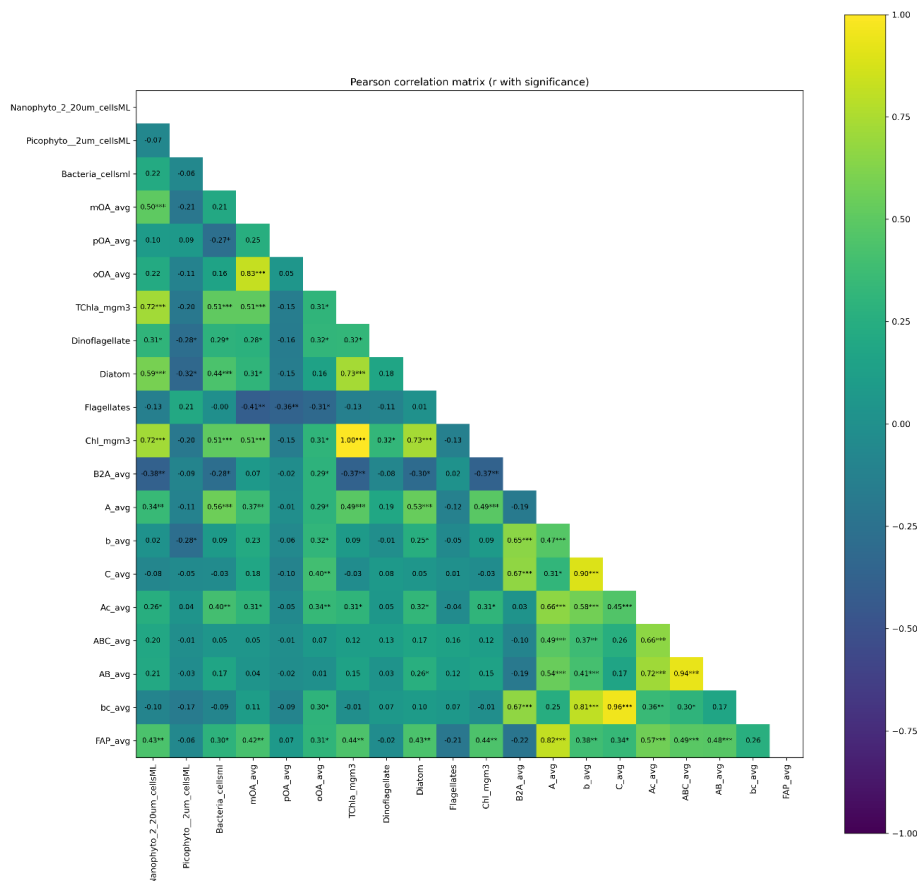


spectrometer, like the WIBS, was used to investigate the biological content of nascent seawater particles (Friestas et al., 2022). In their study, Friestas et al., (2022), focused on comparing online nascent sea spray particles fluorescent signals, to both bulk seawater and primary sea spray aerosol biology measurements. Using online spectroscopy only a small fraction of particles was observed to have fluorescent properties, it was suggested that not all biological species will fluoresce at the wavelengths used in the online spectrometers, and that in addition, bacterial species are selectively aerosolised and not representative of the bulk seawater. In the present study we take a similar approach, examining specific relationships between the different fluorescent channels.

#### 4.2 Co-variability of relations between nascent aerosol fluorescent properties and seawater biogeochemistry.

As already presented, several seawater and nascent seawater aerosols properties were measured during this study including seawater biogeochemistry, and nascent seawater aerosol physical, chemical and fluorescent properties. Correlations were investigated for each of the fluorescing channels of the WIBS, as well as the ratios between these channels (B2A) (Fig. 5). For seawater biochemistry, significant positive correlations were observed between Chl-a, nanophytoplankton, bacterial cells, and diatoms were all well correlated with particles fluorescing in the A channels ( $r=0.49$ ,  $r=0.34$ ,  $r=0.56$ , and  $r=0.53$ ), and with MOA ( $R=0.51$ ,  $R=0.50$ ,  $R=0.21$ ,  $R=0.53$   $p<0.01$  respectively). These correlations may arise from these biological species being increased in FW waters, as MOA is. Nanophytoplankton have already been related to increases in particle number concentrations and MOA (Sellegrì et al., 2021). In this data set, MOA showed significant positive correlations with A-type particles, as well as with Chl-a, bacterial cells and nanophytoplankton, suggesting that this factor is representative of a nascent biological aerosols derived from oceanic bacteriological processes, in line with previous observations (Freny et al., 2021, Wang et al., 2017). The mechanisms of this relationship are not yet fully understood, although indications that MOA is surface active and enriched in the bubble films, changing the film thickness and lifetime (Freny et al., 2021, Sellegrì et al 2021). Opposite to MOA, the OOA fraction is lowest in the FW and highest in STW and MW, indicating a different processing type. OOA does not show any relationship to the phytoplanktonic groups except a slight anticorrelation to flagellates, a phytoplanktonic group that is increased in FW and MW. These seawater types are also more exposed to sunlight, so the OOA might be indicative of more photochemical processing than MOA, like the observations by Long et al., (2014), an alternative for increased more bacterial degradation than metabolic transformation.

These correlations are also consistent with previous studies that have linked A-type fluorescent particles to bacterial bioaerosol (Sauvage et al., 2017). Interestingly, despite containing signatures for amino acids, the POA did not illustrate any significant correlations with either the fluorescent channels or biological parameters. This may indicate that POA is representative of the aged biologically refractory dissolved organic carbon (DOC) in the ocean. It did, however, have moderate negative correlations with flagellate species ( $r=-0.36$ ).



375

Figure 5: Pearsons r correlations of seawater biogeochemistry, organic aerosol, and fluorescence properties. The significance of correlations are indicated by \* (\* p < 0.05, \*\* p < 0.01, \*\*\* p < 0.001).

380

The FAP correlated with most biological species, diatoms (r= 0.43), Chl-a (r=0.44) but also with nanophytoplankton (r=0.43) and bacteria cells (r= 0.30). It is also correlated to the organic content of the nascent sea spray: the correlation with MOA (r=0.42) and to a lesser extent OOA (r=0.31) is of similar significance than with biological components. Suggesting again that MOA and OOA being themselves of biological origin. The FAP is however un-correlated to POA, indicating that POA is less indicative of biological debris than aged refractory organic matter as suggested earlier. The FAP is dominated by the A channel and therefore highly correlated to the A channel. However, this channel (A) shows slightly different correlations compared to the total FAP with highest correlations found with bacteria (r=0.56) and diatoms (r=0.53) and lower with nanophytoplankton (r=0.34). Channels B and C are found uncorrelated to any marine microorganisms, but are correlated to OOA. Therefore these channels may be sensitive to fluorescing, photochemically produced organic matter. Channel ABC supposedly specifically indicative of biological aerosol is uncorrelated to any marine microorganisms nor Chl-a as well.

390



An additional parameter that can be used to identify the source of fluorescent particles is the ratio of the B to A channel. This ratio is referred to as the humification index and can be used to distinguish protein-derived organic matter from more humic-like material (Moellimi et al., (2021)

395 It is based on the observation that protein-like organic matter typically emits at shorter wavelengths (those corresponding to A), while humified or aromatic organic material tends to emit at longer wavelength ranges (B). Using the WIBS-5, channel B corresponds to a wavelength range from 420 to 650 nm, while channel A covers 310 nm up to 400 nm. Moellimi et al., (2021) measured B2A ratios for ambient Antarctic aerosols ranging from 0.4 up to 5, with high values measured close to Islands with large colonies of penguins, where aromatic organic species were expected, while low values were measured in the open ocean. In this work, B2A ratios measured in  
400 nascent marine aerosols were low and varied from 0.1 up to 2 for fluorescent particles measured at 3  $\delta$ , with an increase of 2 observed during the STW period. For hyperfluorescent particles (at 9  $\delta$ ), values in the STW increased up to 10. These high values were only observed in the STW, suggesting a greater contribution of humic or aromatic-type particles in those particles than in the other regions. In line with this, we observe that this B to A ratio is inversely correlated to nanophyto ( $r=-0.58$ ) and Chl-a ( $r=-0.46$ ).

405 In the STW, nutrients such as nitrogen and phosphorus were lower than in other seawater types, in these nutrient poor waters we can expect some form of microbial degradation of the organic debris resulting in the formation of humic organic matter (Omori et al., 2020). Chlorophyll remained low during this time as did other biological species (Bacterial Cells, nanophytoplankton). Correspondingly, the B2A ratio is anticorrelated with total nitrogen (TN)  $R=-0.48$  ( $p=0.01$ ), nanophytoplankton ( $r=-0.58$ ,  $p=0.001$ ) and bacterial species ( $r=-0.43$ ,  $p=0.001$ ). In  
410 addition, the calculated DI, for the combination of amino acids, was most negative in the STW and was anticorrelated with B2A ( $-0.43$ ,  $p=0.01$ ) (Fig 5), suggesting a higher degradation state and eventually an increase in aromatic or oxidized organic aerosols. This conclusion is supported by the positive correlations between the ratio B2A and OOA (0.29).

This degradation of organic matter in marine seawater resulting in a change in fluorescent properties was also  
415 observed in marine samples at several different depths of seawater (Omori et al., 2020). This was in large part related to the photodegradation of marine biological samples. In the STW, seawater is exposed to much higher levels of sunlight compared to that in the FW or SAW, therefore this change in marine properties can also be a result of the contribution of photobleaching processes.

## 5.0 Conclusions and atmospheric implications

420 This work represents data collected during the 2-week Sea2Cloud cruise ranging from  $-42^\circ$  to  $-47^\circ$  off the coast of New Zealand, through three different water masses. These observations highlight the complexity of the nature of nascent seawater aerosol particles and illustrate strong interactions with seawater biogeochemistry.

The chemical composition of the nascent aerosols, measured with a TASCAM, was dominated by organic material  
425 containing signatures of different biological origin, including amino acids. This organic matter contributed  $35\% \pm 20\%$  to the total submicron mass, containing signatures for both nascent and secondary organic aerosols (OOA and MOA). The presence of oxidized organic material in generated sea spray aerosols suggest that ocean biology can contribute not only to nascent marine aerosols but also to the secondary organic aerosols, with important implications when interpreting aerosol sources in marine environments and for indirect aerosol radiative effects.



430 Given the biological origin of these organic aerosols, they may also represent an important source of ice nucleating particles.

Using WIBS fluorescence measurements several fluorescent channels could be associated with different biological species and illustrate how nascent aerosol fluorescence properties vary with key biological indicators in seawater including Nanophytoplankton, Chl-a, and total bacterial cells. These measurements provide evidence, in a controlled environment, of the associations between seawater biology and nascent sea spray aerosol composition and provides additional evidence that ocean biogeochemistry can directly influence marine aerosol properties. It also highlights the need to integrate biology, chemistry and physics when studying processes at the ocean atmospheric interface. The combination of continuous measurements of fluorescence, mass spectral and biology and evolving seawater masses, provides a powerful approach to trace biological activity and provides new parameters that can be considered in climate models.

## 6.0 References

- Alfarra, M. R., Coe, H., Allan, J. D., Bower, K. N., Boudries, H., Canagaratna, M. R., Jimenez, J. L., Jayne, J. T., Garforth, A. A., Li, S., & Worsnop, D. R. (2004). Characterization of urban and rural organic particulate in the Lower Fraser Valley using two Aerodyne Aerosol Mass Spectrometers. *Atmospheric Environment*, 38(34), 5745-5758.
- Barthelmeß, T., Cristi, A., Deppeler, S., Safi, K., Sellegri, K., Law, C. S., & Engel, A. (2024). Pronounced Diel Cycling of Dissolved Carbohydrates and Amino Acids in the Surface Ocean and across Diverse Regimes. *Environmental Science & Technology*, 59(1), 419-429. <https://doi.org/10.1021/acs.est.4c00491>
- 445 Bigg, E. K., & Leck, C. (2008). The composition of fragments of bubbles bursting at the ocean surface. *Journal Of Geophysical Research*, 113(D11). <https://doi.org/10.1029/2007jd009078>
- Blanchard, D. C., & Woodcock, A. H. (1957). Bubble Formation and Modification in the Sea and its Meteorological Significance. *Tellus*, 9(2), 145-158.
- Brean, J., Dall'Osto, M., Simó, R., Shi, Z., Beddows, D. C. S., & Harrison, R. M. (2021). Open ocean and coastal new particle formation from sulfuric acid and amines around the Antarctic Peninsula. *Nature Geoscience*, 14(6), 383-388. <https://doi.org/10.1038/s41561-021-00751-y>
- Chevassus, E., Fossum, K. N., Ceburnis, D., Lei, L., Lin, C., Xu, W., O'Dowd, C., & Ovadnevaite, J. (2025). Marine organic aerosol at Mace Head : effects from phytoplankton and source region variability. *Atmospheric Chemistry And Physics*, 25(7), 4107-4129.
- 460 Chen, B., Lei, L., Chevassus, E., Xu, W., Zhen, L., Zhong, H., Wang, L., Lin, C., Huang, R.-J., Ceburnis, D., O'Dowd, C., and Ovadnevaite, J.: Differentiation of primary and secondary marine organic aerosol with machine learning, *EGUsphere [preprint]*, <https://doi.org/10.5194/egusphere-2025-1415>, 2025.
- Chiswell, S. M., Bostock, H. C., Sutton, P. J., & Williams, M. J. (2015). Physical oceanography of the deep seas around New Zealand: a review. *New Zealand Journal of Marine and Freshwater Research*, 49(2), 286-317. <https://doi.org/10.1080/00288330.2014.992918>
- 465 Crawford, I., Gallagher, M. W., Bower, K. N., Choularton, T. W., Flynn, M. J., Ruske, S., Listowski, C., Brough, N., Lachlan-Cope, T., Fleming, Z. L., Foot, V. E., & Stanley, W. R. (2017). Real-time detection of airborne fluorescent bioparticles in Antarctica. *Atmospheric Chemistry And Physics*, 17(23), 14291-14307.



- 470 Dauwe, B., Middelburg, J. J., Herman, P. M. J., & Heip, C. H. R. (1999). Linking diagenetic alteration of amino acids and bulk organic matter reactivity. *Limnology And Oceanography*, 44(7), 1809-1814.
- Decesari, S., Finessi, E., Rinaldi, M., Paglione, M., Fuzzi, S., Stephanou, E. G., Tziaras, T., Spyros, A., Ceburnis, D., O'Dowd, C., Dall'Osto, M., Harrison, R. M., Allan, J., Coe, H., & Facchini, M. C. (2011). Primary and secondary marine organic aerosols over the North Atlantic Ocean during the MAP experiment. *Journal Of Geophysical Research Atmospheres*, 116(D22), n/a. <https://doi.org/10.1029/2011jd016204>
- 475 Decesari, S., Paglione, M., Rinaldi, M., Dall'Osto, M., Simó, R., Zanca, N., Volpi, F., Facchini, M. C., Hoffmann, T., Götz, S., Kampf, C. J., O'Dowd, C., Ceburnis, D., Ovadnevaite, J., & Tagliavini, E. (2020). Shipborne measurements of Antarctic submicron organic aerosols : an NMR perspective linking multiple sources and bioregions. *Atmospheric Chemistry And Physics*, 20(7), 4193-4207.
- Facchini, M. C., Rinaldi, M., Decesari, S., Carbone, C., Finessi, E., Mircea, M., Fuzzi, S., Ceburnis, D., Flanagan, R., Nilsson, E. D., De Leeuw, G., Martino, M., Woeltjen, J., & O'Dowd, C. D. (2008). Primary submicron marine aerosol dominated by insoluble organic colloids and aggregates. *Geophysical Research Letters*, 35(17).
- Flato, G. M., Marotzke, J., Abiodun, B., Braconnot, P., Chou, S. C., Collins, W., et al. (2013). Evaluation of climate models. *Climate change 2013 – the physical science basis: Working group I contribution to the fifth assessment report of the intergovernmental panel on climate change*. Cambridge University Press. Retrieved from
- 485 Freitas, G. P., Stolle, C., KFrohlaye, P. H., Stanley, W., Herlemann, D. P. R., Salter, M. E., & Zieger, P. (2022). Emission of primary bioaerosol particles from Baltic seawater. *Environmental Science. Atmospheres*, 2(5), 1170-1182. <https://doi.org/10.1039/d2ea00047d>
- Freney, E., and Coauthors, 2021: Mediterranean nascent sea spray organic aerosol and relationships with seawater biogeochemistry. *Atmos. Chem. Phys.*, 21, 10 625–10 641, .
- 490 Fuentes, E., H. Coe, D. Green, G. de Leeuw, and G. McFiggans, 2010: On the impacts of phytoplankton-derived organic matter on the properties of the primary marine aerosol—Part 1: Source fluxes. *Atmos. Chem. Phys.*, 10, 9295–9317, <https://doi.org/10.5194/acp-10-9295-2010>.
- Gabey, A. M., Gallagher, M. W., Whitehead, J., Dorsey, J. R., Kaye, P. H., & Stanley, W. R. (2010). Measurements and comparison of primary biological aerosol above and below a tropical forest canopy using a dual channel fluorescence spectrometer. *Atmospheric Chemistry And Physics*, 10(10), 4453-4466. <https://doi.org/10.5194/acp-10-4453-2010>
- 495 Hernandez, M., Perring, A. E., McCabe, K., Kok, G., Granger, G., & Baumgardner, D. (2016). Chamber catalogues of optical and fluorescent signatures distinguish bioaerosol classes. *Atmospheric Measurement Techniques*, 9(7), 3283-3292.
- 500 Hodshire, A. L., Campuzano-Jost, P., Kodros, J. K., Croft, B., Nault, B. A., Schroder, J. C., Jimenez, J. L., & Pierce, J. R. (2019). The potential role of methanesulfonic acid (MSA) in aerosol formation and growth and the associated radiative forcings. *Atmospheric Chemistry And Physics*, 19(5), 3137-3160. <https://doi.org/10.5194/acp-19-3137-2019>
- Hill, S. C., Pinnick, R. G., Niles, S., Pan, Y., Holler, S., Chang, R. K., Bottiger, J., Chen, B. T., Orr, C., & Feather, G. (1999). Real-time measurement of fluorescence spectra from single airborne biological particles. *Field Analytical Chemistry & Technology*, 3(4-5), 221-239. [https://doi.org/10.1002/\(sici\)1520-6521\(1999\)3:4/5](https://doi.org/10.1002/(sici)1520-6521(1999)3:4/5)
- 505



- Kawana, K., Matsumoto, K., Taketani, F., Miyakawa, T., and Kanaya, Y.: Fluorescent biological aerosol particles over the central Pacific Ocean: covariation with ocean surface biological activity indicators, *Atmos. Chem. Phys.*, 21, 15969–15983, <https://doi.org/10.5194/acp-21-15969-2021>, 2021.
- 510 Kawana, K., Taketani, F., Matsumoto, K., Tobo, Y., Iwamoto, Y., Miyakawa, T., Ito, A., and Kanaya, Y.: Roles of marine biota in the formation of atmospheric bioaerosols, cloud condensation nuclei, and ice-nucleating particles over the North Pacific Ocean, Bering Sea, and Arctic Ocean, *Atmos. Chem. Phys.*, 24, 1777–1799, <https://doi.org/10.5194/acp-24-1777-2024>, 2024.
- Lohmann, U., & Lesins, G. (2002). Stronger Constraints on the Anthropogenic Indirect Aerosol Effect. *Science*, 298(5595), 1012-1015. <https://doi.org/10.1126/science.1075405>
- 515 Lewis, R., & Schwartz, E. (2004). Sea Salt Aerosol Production : Mechanisms, Methods, Measurements and Models—A Critical Review. Dans *Geophysical monograph*. <https://doi.org/10.1029/gm152>
- Long, M. S., Keene, W. C., Kieber, D. J., Frossard, A. A., Russell, L. M., Maben, J. R., Kinsey, J. D., Quinn, P. K., & Bates, T. S. (2014). Light-enhanced primary marine aerosol production from biologically productive seawater. *Geophysical Research Letters*, 41(7), 2661-2670. <https://doi.org/10.1002/2014gl059436>
- 520 Moallemi, A., Landwehr, S., Robinson, C., Simó, R., Zamanillo, M., Chen, G., et al. (2021). Sources, occurrence and characteristics of fluorescent biological aerosol particles measured over the pristine Southern Ocean. *Journal of Geophysical Research: Atmospheres*, 126, e2021JD034811.
- Moore, A. N., Cancelada, L., Kimble, K. A., & Prather, K. A. (2024). Secondary aerosol formation from mixtures of marine volatile organic compounds in a potential aerosol mass oxidative flow reactor. *Environmental Science Atmospheres*, 4(3), 351-361. <https://doi.org/10.1039/d3ea00169e>
- 525 Omori, Y., Saeki, A., Wada, S., Inagaki, Y., & Hama, T. (2020). Experimental Analysis of Diurnal Variations in Humic-Like Fluorescent Dissolved Organic Matter in Surface Seawater. *Frontiers In Marine Science*, 7. <https://doi.org/10.3389/fmars.2020.589064>
- 530 Ovadnevaite, J., Čeburnis, D., Martucci, G., Bialek, J., Monahan, C., Rinaldi, M., Facchini, M. C., Berresheim, H., Worsnop, D. R., & O'Dowd, C. (2011a). Primary marine organic aerosol : A dichotomy of low hygroscopicity and high CCN activity. *Geophysical Research Letters*, 38(21), n/a.
- Ovadnevaite, J., O'Dowd, C., Dall'Osto, M., Čeburnis, D., Worsnop, D. R., & Berresheim, H. (2011b). Detecting high contributions of primary organic matter to marine aerosol : A case study. *Geophysical Research Letters*, 38(2), n/a. <https://doi.org/10.1029/2010gl046083>
- 535 Patterson, J. P., Collins, D. B., Michaud, J. M., Axson, J. L., Sultana, C. M., Moser, T., Dommer, A. C., Conner, J., Grassian, V. H., Stokes, M. D., Deane, G. B., Evans, J. E., Burkart, M. D., Prather, K. A., & Gianneschi, N. C. (2016). Sea Spray Aerosol Structure and Composition Using Cryogenic Transmission Electron Microscopy. *ACS Central Science*, 2(1), 40-47. <https://doi.org/10.1021/acscentsci.5b00344>
- 540 Perring, A. E., Schwarz, J. P., Baumgardner, D., Hernandez, M. T., Spracklen, D. V., Heald, C. L., Gao, R. S., Kok, G., McMeeking, G. R., McQuaid, J. B., & Fahey, D. W. (2015). Airborne observations of regional variation in fluorescent aerosol across the United States. *Journal Of Geophysical Research. Atmospheres*, 120(3), 1153-1170. <https://doi.org/10.1002/2014jd022495>
- 545 Savage, N. J., Krentz, C. E., Könemann, T., Han, T. T., Mainelis, G., Pöhlker, C., & Huffman, J. A. (2017). Systematic characterization and fluorescence threshold strategies for the wideband integrated bioaerosol sensor



- (WIBS) using size-resolved biological and interfering particles. *Atmospheric Measurement Techniques*, 10(11), 4279–4302.
- Schmale, J., Schneider, J., Nemitz, E., Tang, Y. S., Dragosits, U., Blackall, T. D., Trathan, P. N., Phillips, G. J., Sutton, M., & Braban, C. F. (2013). Sub-Antarctic marine aerosol : dominant contributions from biogenic sources. *Atmospheric Chemistry And Physics*, 13(17), 8669-8694. <https://doi.org/10.5194/acp-13-8669-2013>
- Schmale, J., Baccarini, A., Thurnherr, I., Henning, S., Efraim, A., Regayre, L., Bolas, C., Hartmann, M., Welti, A., Lehtipalo, K., Aemisegger, F., Tatzelt, C., Landwehr, S., Modini, R. L., Tummon, F., Johnson, J., Harris, N., Schnaiter, M., Toffoli, A., Derkani, M., Bukowiecki, N., Stratmann, F., Dommen, J., Baltensperger, U., Wernli, H., Rosenfeld, D., Gysel-Beer, M., and Carslaw, K.: Overview of the Antarctic Circumnavigation Expedition: Study of Preindustrial-like Aerosols and Their Climate Effects (ACE-SPACE), *Bulletin of the American Meteorological Society*, 0, null, <https://doi.org/10.1175/BAMS-D-18-0187.1>, 2019.
- Schwier, A. N., Rose, C., Asmi, E., Ebling, A. M., Landing, W. M., Marro, S., Pedrotti, M., Sallon, A., Iuculano, F., Agusti, S., Tsiola, A., Pitta, P., Louis, J., Guieu, C., Gazeau, F., & Sellegri, K. (2015). Primary marine aerosol emissions from the Mediterranean Sea during pre-bloom and oligotrophic conditions : correlations to seawater chlorophyll & ; It ; i& ; gt ; a& ; It ; /i& ; gt ; from a mesocosm study. *Atmospheric Chemistry And Physics*, 15(14), 7961-7976. <https://doi.org/10.5194/acp-15-7961-2015>
- Sellegri, K., Barthelmeß, T., Trueblood, J., Cristi, A., Freney, E., Rose, C., Barr, N., Harvey, M., Safi, K., Deppeler, S., Thompson, K., Dillon, W., Engel, A., and Law, C.: Quantified effect of seawater biogeochemistry on the temperature dependence of sea spray aerosol fluxes, *Atmos. Chem. Phys.*, 23, 12949–12964, <https://doi.org/10.5194/acp-23-12949-2023>, 2023a
- Sellegri, K., Harvey, M., Peltola, M., Saint-Macary, A., Barthelmeß, T., Rocco, M., Moore, K. A., Cristi, A., Peyrin, F., Barr, N., Labonnote, L., Marriner, A., McGregor, J., Safi, K., Deppeler, S., Archer, S., Dunne, E., Harnwell, J., Delanoe, J., . . . Law, C. S. (2023b). Sea2Cloud : From Biogenic Emission Fluxes to Cloud Properties in the Southwest Pacific. *Bulletin of the American Meteorological Society*, 104(5), E1017-E1043. <https://doi.org/10.1175/bams-d-21-0063.1>
- Sellegri, K., Nicosia, A., Freney, E., Uitz, J., Thyssen, M., Grégori, G., Engel, A., Zäncker, B., Haëntjens, N., Mas, S., Picard, D., Saint-Macary, A., Peltola, M., Rose, C., Trueblood, J., Lefevre, D., D’Anna, B., Desboeufs, K., Meskhidze, N., . . . Law, C. S. (2021). Surface ocean microbiota determine cloud precursors. *Scientific Reports*, 11(1).
- Seinfeld, J. H., and Pandis, S. N. (2016). *Atmospheric Chemistry and Physics: From Air Pollution to Climate Change* (3rd ed.). John Wiley & Sons, Hoboken, NJ.
- Shulman, M. L., Charlson, R. J., & Davis, E. J. (1997). The effects of atmospheric organics on aqueous droplet evaporation. *Journal Of Aerosol Science*, 28(5), 737-752.
- Timonen, H., Cubison, M., Aurela, M., Brus, D., Lihavainen, H., Hillamo, R., Canagaratna, M., Nekat, B., Weller, R., Worsnop, D., & Saarikoski, S. (2016). Applications and limitations of constrained high-resolution peak fitting on low resolving power mass spectra from the ToF-ACSM. *Atmospheric Measurement Techniques*, 9(7), 3263-3281. <https://doi.org/10.5194/amt-9-3263-2016>
- Wang, X., Deane, G. B., Moore, K. A., Ryder, O. S., Stokes, M. D., Beall, C. M., Collins, D. B., Santander, M. V., Burrows, S. M., Sultana, C. M., & Prather, K. A. (2017). The role of jet and film drops in controlling the



585 mixing state of submicron sea spray aerosol particles. *Proceedings Of The National Academy Of Sciences Of The United States Of America*, 114(27), 6978-6983.

Wang, X., Sultana, C. M., Trueblood, J., Hill, T. C. J., Malfatti, F., Lee, C., Laskina, O., Moore, K. A., Beall, C. M., McCluskey, C. S., Cornwell, G. C., Zhou, Y., Cox, J. L., Pendergraft, M. A., Santander, M. V., Bertram, T. H., Cappa, C. D., Azam, F., DeMott, P. J., . . . Prather, K. A. (2015). Microbial Control of Sea Spray Aerosol Composition : A Tale of Two Blooms. *ACS Central Science*, 1(3), 124-131. <https://doi.org/10.1021/acscentsci.5b00148>

590 Wilson, T. W., Ladino, L. A., Alpert, P. A., Breckels, M. N., Brooks, I. M., Browse, J., Burrows, S. M., Carslaw, K. S., Huffman, J. A., Judd, C., Kilhau, W. P., Mason, R. H., McFiggans, G., Miller, L. A., Nájera, J. J., Polishchuk, E., Rae, S., Schiller, C. L., Si, M., . . . Murray, B. J. (2015). A marine biogenic source of atmospheric ice-nucleating particles. *Nature*, 525(7568), 234-238.

Wohl, C., Li, Q., Cuevas, C. A., Fernandez, R. P., Yang, M., Saiz-Lopez, A., & Simó, R. (2023). Marine biogenic emissions of benzene and toluene and their contribution to secondary organic aerosols over the polar oceans. *Science Advances*, 9(4).

600 Zhou, X., Davis, A. J., Kieber, D. J., Keene, W. C., Maben, J. R., Maring, H., Dahl, E. E., Izaguirre, M. A., Sander, R., & Smoydzyn, L. (2008). Photochemical production of hydroxyl radical and hydroperoxides in water extracts of nascent marine aerosols produced by bursting bubbles from Sargasso seawater. *Geophysical Research Letters*, 35(20). <https://doi.org/10.1029/2008gl035418>

## 605 **7.0 Acknowledgements**

This research received funding from the European Research Council (ERC) under the Horizon 2020 research and innovation programme (Grant Agreement 771369), the Centre National des Etudes Spatiales (CNES), and was supported by NIWA SSIF funding to the Ocean-Climate Interactions, and Flows and Productivity Programmes. The authors wish to acknowledge Cliff Law of NIWA for providing the cytometry flow data from the seawater.

610 We acknowledge the support and expertise of the Officers and Crew of the R/V *Tangaroa* and NIWA Vessel Services. The Sea2Cloud project is endorsed by SOLAS.